Comptes Rendus

Chimie

Manuel Horue, Facundo Barraqué, María Luciana Montes, María Emilia Zelaya-Soulé, César Fernández Morantes, Florencia Camila Urruchua, Hilda Edith Correa, Guillermo Raul Castro and Mariela Alejandra Fernandez

Development of antibacterial magnetic clay-based nanocomposites for water treatment

ACADÉMIE
DES SCIENCES
INSTITUT DE FRANCE

Research article

Development of antibacterial magnetic clay-based nanocomposites for water treatment

Manuel Horue [®,a], **Facundo Barraqué** [®,b], **María Luciana Montes** [®,c], **María Emilia Zelaya-Soulé** [®,d], **César Fernández Morantes** [e], **Florencia Camila Urruchua** [®,b], **Hilda Edith Correa** [b], **Guillermo Raul Castro** [®,f,g] and **Mariela Alejandra Fernandez** [®,*,b]

[a] Centro de Investigación y Desarrollo en Fermentaciones Industriales (CINDEFI), Laboratorio de Nanobiomateriales, Departamento de Química, Facultad de Ciencias Exactas, Universidad Nacional de La Plata-CONICET (CCT La Plata), Calle 47 y 115, B1900AJL La Plata, Argentina

[b] CETMIC, Camino Centenario y 506, B1897ZCA M. B. Gonnet, Argentina

[c] IFLP, Instituto de Física La Plata - CONICET CCT-La Plata, Departamento de Física, Facultad de Ciencias Exactas, Universidad Nacional de La Plata, Argentina

[d] INEDES - CONICET CCT Oca Centenario, Universidad Nacional de Luján, Luján, Argentina

[e] Grupo de Investigación en Tecnologías y Ambiente (GITA), Corporación Universitaria Autónoma del Cauca, Calle 5 No. 3-85, 190003, Popayán, Colombia

[f] Max Planck Laboratory for Structural Biology, Chemistry and Molecular Biophysics of Rosario (MPLbioR, UNR-MPIbpC). Partner Laboratory of the Max Planck Institute for Biophysical Chemistry (MPIbpC, MPG). Centro de Estudios Interdisciplinarios (CEI), Universidad Nacional de Rosario, Maipú 1065, S2000 Rosario, Santa Fe, Argentina

[g] Nanomedicine Research Unit (Nanomed), Center for Natural and Human Sciences (CCNH), Universidade Federal do ABC (UFABC), Santo André, SP, Brazil

E-mail: marielafernandez0712@gmail.com (M. A. Fernandez)

Abstract. Organoclays were prepared using Argentinean montmorillonite (Mt), hexadecyltrimethylammonium, or benzalkonium chloride at different concentrations. Surfactant incorporation, a key factor in biocide capacity, was estimated using interlayer space and thermogravimetric analysis (TGA). Subsequently, Fe oxides were grown on the organoclays. Saturation magnetization indicated that all magnetic composites could respond to an external magnetic field. Inhibition experiments showed high antibacterial activity against *Enterococcus faecium*, *Escherichia coli*, and *Salmonella typhimurium*. The synthesized nanocomposites loaded with 150% CEC (cation exchange capacity) of hexadecyltrimethylammonium were the most effective. Those results were more precisely investigated using the viable plate count method. The magnetic materials had a similar antimicrobial effect to those without magnetic properties, indicating that Fe oxides can be nucleated to impart a magnetic response without affecting the biocide properties. The organoclays showed higher antibacterial activity against *E. coli* than against the other bacteria assayed. In addition, the agar disk-diffusion method

---

* Corresponding author.

revealed that antimicrobial agents were not released from clays, which is a relevant fact in the water treatment process.

1. Introduction

In different parts of the world, drinking water usually contains a diversity of pathogens, such as viruses, bacteria, protozoa, and parasites, which pose a serious risk to human health. In particular, gram-negative bacteria (*S. typhimurium*, *E. coli*, *Vibrio cholera*, and *Campylobacter jejuni*) and some gram-positive bacteria (*Bacillus cereus*, and *Staphylococcus aureus*) have been reported as harmful microorganisms found in the water of different countries, and the monitoring and remediation of water containing them is crucial to avoid associated complications related to the most predominant pathogens mentioned above [1]. This is necessary and encourages the production of simple and economical materials to address this problem.

Several biocide materials based on clays, such as clays modified by the sorption of biocide compounds, have been proposed for various applications, including cosmetics, medicine, food, and the detergent industry [2]. Among biocide compounds, alkyltrimethylammonium cations, especially quaternary amines, are commonly employed as organic compounds with antibacterial activity [3–6]. However, the isolated use of these compounds for wastewater treatment is limited because they are soluble and can become pollutants in the effluent. Therefore, the employment of adequate support materials that allow the biocide action of the compounds to avoid their dissolution in the effluent is a potential alternative.

Clays have been proposed as support materials for biocidal compounds. Among them, those based on montmorillonite (Mt) and alkyltrimethylammonium cations have been proposed as antifungal materials [6,7] and pollutant adsorption materials [8,9]. More recently, organoclays with a magnetic response, that is, organoclays modified by the growth of magnetic Fe oxide particles, have also been employed for the removal of heavy metals, dyes, and arsenic [10–12]. The combination of magnetic nanoparticles with clays has been considered for enzymatic immobilization [13,14], the development of catalytic materials [15,16], environmental remediation [17–20], and the design of biocompatible materials [21]. With regard to water treatment, these materials have the advantage of providing new sorption sites, but also allowing material recuperation through magnetic external fields. It avoids direct handling and decreases the health risk of workers. However, the antibacterial capacity of these materials and the potential changes caused by Fe growth have not yet been analyzed.

The demonstration of antibacterial activity by magnetic organoclays will allow us to obtain magnetic and biocidal materials in a single composite. This study aimed to provide an overview of antibacterial activity against gram-positive and gram-negative bacteria of magnetic organoclays, synthesized by the incorporation of hexadecyltrimethylammonium or benzalkonium chloride on an Argentinean Mt, with posterior Fe oxide nucleation.

2. Materials and methods

2.1. *Materials*

Commercial Argentinean bentonite (Castiglioni Pes and Co.) from *Río Negro* Province was used as raw material. The main bentonite component is montmorillonite (Mt) (88.2%) with structural formula $(Si_{3.81}Al_{0.19})(Al_{1.40}Fe^{3+}_{0.27}Mg_{0.32})10(OH)_2Na_{0.37}Ca_{0.06}K_{0.02}$ [6]. The bentonite has an isoelectric point at pH 2.7, the external surface area (determined by N_2 adsorption) is 66.0 m^2/g [19], and its cation exchange capacity (CEC) of 0.825 mmol/g [22].

The surfactants used for organoclay synthesis were hexadecyltrimethylammonium bromide (HDTMABr) or benzalkonium chloride (BAC). HDTMABr (Purity > 97%, MW = 364.45 g/mol, and critical micelle concentrations of 0.9 mM) was provided by Fluka (Buchs, Switzerland). BAC (95% purity, MW_{avg} = 354 g/mol, being a mixture of alkylbenzyldimethylammonium chlorides with alkyl chains of C8, C10, C12, C14, C16, and C18 length) was purchased from Sigma (Buenos Aires, Argentina).

The KNO_3 and KOH (99% purity) used for Fe oxides synthesis were purchased from Biopack, while
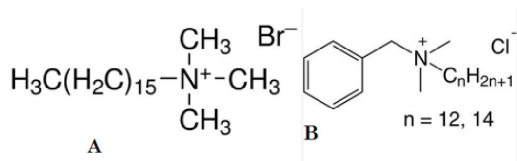
Figure 1. Chemical structures of HDTMABr (A) and BAC (B).

Fe $(SO_4) \cdot 7H_2O$ (analytical degree) was supplied from Cicarelli Lab (Buenos Aires, Argentina).

Escherichia coli ATCC 25922, *Enterococcus faecium*, and *Salmonella typhimurium* were donated by the Microbiology Department, School of Sciences, *Universidad Nacional de* La Plata (Argentina).

Nutrient broth, nutrient agar, and Mueller Hinton (MH) agar were purchased from Merck (Darmstadt, Germany), and resazurin from Sigma (Buenos Aires, Argentina). Ultrapure water (Milli-Q grade, 0.22 μm filtered) was employed to prepare all media and dispersions (Millipore Co., MA, USA).

2.2. *Materials synthesis*

Organoclays were produced in batch conditions by putting in contact with 15 g of Mt and solutions of HDTMABr or BAC (1 L) with concentrations equivalent to 50%, 100%, or 150% to the bentonite CEC. The suspensions were stirred at 400 rpm for 24 h (room temperature). The obtained products were washed several times with distilled water, lyophilized, ground, and adequately stored. The synthesized products were labeled with prefixes H, for bentonite modified by HDTMABr, (Figure 1A) or B when BAC (Figure 1B) was used, followed by the surfactant concentration in solution (50, 100, or 150) and finally by Mt from montmorillonite (i.g.: H50Mt).

Magnetic organoclay was synthesized following a previously reported procedure [11,23], using the organoclays as base materials. For this, 25 mL of 0.3 M $FeSO_4 \cdot 7H_2O$ solution was incorporated into an organoclay suspension (5.9 g/L water) and kept under continuous shaking for 2 h. Then 25 mL of 0.49 M KNO_3 solution and 25 mL of 1.25 M KOH solution were added, and the suspension was heated to 90 °C for 2 min. The system was cooled to room temperature and the obtained material was washed twice with distilled water. The samples were recovered by magnetic separation and lyophilized. The materials were labeled as the organoclays base material but adding Mag at the end of the name (e.g., H50MtMag). The synthesis was replicated using raw clay instead of organoclay, and the material was labeled MtMag.

2.3. *Samples characterization*

X-ray diffraction (XRD) patterns were measured using a Philips PW 1710 diffractometer (CuKα radiation, 40 kV, 35 mA, 10 s/step, 0.02° step size). To improve the diffraction peak definition corresponding to the crystallographic plane 001 of Mt, samples were scanned in oriented mode. For this, samples were previously maintained at 0.47 relative humidity for 48 h.

Thermogravimetric measurements (TGA) were performed using Rigaku 8121 equipment, with alumina as reference material. For that, 20 mg of samples were placed on alumina crucibles and heated from 24 °C to 1000 °C, in an air atmosphere, increasing the temperature at a rate of 10 °C/min. The TGA first-order derivative (DTGA) was calculated. The actual surfactant loaded was determined, with respect to the clay CEC, considering the mass loss between 150 °C and 1000 °C, as previously reported [6].

The Mössbauer spectra of Mag samples were measured at room temperature employing a spectrometer, in transmission geometry, containing a ^{57}Co/Rh radioactive source (constant acceleration, 512 multichannel detections). A 12 μm thick α-Fe foil was used for velocity calibration and all the isomer shifts were referred to this standard. Each Mössbauer spectrum was analyzed using a commercial program that allows the use of a hyperfine magnetic field and quadrupole splitting distributions [24]. The total Fe concentration of the samples was estimated from the Mössbauer spectrum, following the procedure proposed by Montes [25].

For hysteresis loops measurements, the samples were placed on a diamagnetic sample holder with a negligible signal. The equipment used was a LakeShore 7404 vibrating sample magnetometer, applying an external field between ±1.9 T. The extracted magnetic parameters were the high field susceptibility (χ_{hifi}), remnant magnetization (Mr), coercive field (Hc), and saturation magnetization (Ms).

2.4. *Antimicrobial assays*

2.4.1. *Microdilution method and minimum inhibitory concentration (MIC)*

Overnight cultures of *E. coli* (ATCC 25922), *S. typhimurium*, and *E. faecium* were cultured in fresh nutrient broth from cell stocks preserved at −80 °C. After incubation, the bacterial concentration was adjusted to 1.0×10^8 cells/mL to produce the inocula.

The bactericidal activity of Mt, MtMag, H50Mt, H50MtMag, H100Mt, H100MtMag, H150Mt, H150MtMag, B50Mt, B50MtMag, B100Mt, B100MtMag, B150Mt, and B150MtMag was evaluated in suspensions of nutrient broth using the microdilution method in 1.5 mL Eppendorf tubes, according to International Clinical Standards. The samples were suspended in 900 μL of nutrient broth at concentrations of 10.0, 5.0, 2.5, 1.25, and 0.625 g/L, and 100 μL of bacterial inoculum was added to each tube. The tubes were incubated in a shaker at 15 rpm at 37 °C for 24 h. Controls were prepared without clays or bacteria. The tubes were decanted after incubation, the supernatants were transferred to a 96-well microtiter plate, and viable cells were quantified by the reduction of the vital dye resazurin assay [26]. Finally, the MIC was determined for each sample.

2.4.2. *Agar disk-diffusion method*

The presence of growth inhibition haloes was assayed to evaluate the extent of biocide activity. The procedure was carried out according to the guidelines described by the International Clinical Standards (CLSI/NCCLS) using sterile glass cylinders of 8 mm 6 mm 10 mm (external and internal diameter, length) containing sample suspensions instead of paper disks. Samples with a relatively high amount of surfactant (H150Mt, H150MtMag, B150Mt, and B150MtMag) were considered for this assay, employing 10 g/L of each suspension, while Mt and MtMag were used as control samples. Overnight cultures of *E. coli*, *S. typhimurium*, and *E. faecium* were used to prepare adjusted inocula of 1.5×10^8 cells/mL and then employed as inoculum to seed MH agar plates. The cylinders were placed after inoculation and 50 μM of each sample was dropped into the respective cylinder. Incubation was carried out at 37 °C for 24 h.

2.4.3. *Assays in Erlenmeyer flasks*

Assays in Erlenmeyer flasks were performed using only the samples with the highest antimicrobial efficiency based on the microdilution method results. The tests were performed in 50-mL Erlenmeyer flasks, and the viable plate count method was used to enumerate viable bacteria.

In this procedure, overnight cultures of each strain were employed as inoculum (1.5×10^8 cells/mL). The assayed materials (H150Mt and H150MtMag) were dispersed in fresh nutrient broth at different concentrations, depending on the susceptibility of each bacterium. Specifically, 0.25 g/L was added to fresh media against *E. coli*, 0.50 g/L against *S. typhimurium*, and 0.80 g/L against *E. faecium*. Bacterial inoculum was added to a final volume of 20 mL. The microdilution method showed that the MtMag samples were harmless to all strains. Based on these results, a control constituted by MtMag was used at the corresponding concentration in all cases. The incubation conditions were 37 °C and orbital shaking at 200 rpm for 24 h. After the incubation period, aliquots were taken from each sample and dilutions ranging from 10^{-1} to 10^{-9} were prepared. The cells were then plated on nutrient agar and incubated at 37 °C for 24 h. Finally, the colony-forming units (CFU) were quantified. All experiments were performed in triplicate.

2.5. *Statistical analysis*

Data obtained from the viable plate count method were graphed and analyzed using GraphPad Prism version 6.00 software (GraphPad). Data related to the number of viable bacteria were analyzed using Student's *t*-test. Differences between groups were considered significant when *p*-values were lower than 0.05 (95% confidence level).

3. Results

3.1. *Sample characterization*

Table 1 shows the d001 values (corresponding to the interlayer space of Mt) for all considered samples. Organic samples presented d001 values higher than those of Mt, which indicated the entrance of the surfactant into the Mt interlayer space. The d001 values,

Table 1. The d001 (nm) and the actual organic load (% CEC, calculated from TGA) indicate the organic content in the external surface (VdW) and the interlayer space (exchanged)

Sample	d001 (nm)	Actual load (% CEC)	VdW (% CEC)	Exchanged (% CEC)
Mt*	1.26 (Na^+) 1.43 (Ca^{2+})	0	0	0
MtMag*	1.27 (Na^+/Fe) 1.47 (Ca^{2+})	0	0	0
H50Mt*	1.5	43 ± 4	23 ± 2	20 ± 2
H100Mt*	2.1	84 ± 7	59 ± 4	25 ± 2
H150Mt*	2.2	116 ± 10	89 ± 8	27 ± 3
H50MtMag*	1.6	36 ± 3	16 ± 2	20 ± 2
H100MtMag*	2.0	68 ± 6	38 ± 3	30 ± 2
H150MtMag*	2.2	90 ± 9	63 ± 6	27 ± 3
B50Mt	1.6	41 ± 4	14 ± 1	27 ± 3
B100Mt	1.8	72 ± 7	52 ± 4	20 ± 2
B150Mt	2.0	79 ± 7	58 ± 6	21 ± 2
B50MtMag	1.6	30 ± 3	23 ± 2	13 ± 1
B100MtMag	1.9	57 ± 6	36 ± 3	21 ± 2
B150MtMag	1.9	36 ± 6	41 ± 4	25 ± 2

Note: Previously reported [11].

previously reported for H50Mt, H100Mt, and H150Mt were 1.5, 2.1, and 2.2 nm, respectively [11], revealing a monolayer arrangement for H50Mt but pseudo-trilayer for the others [27,28]. Similar d001 values and surfactant arrangements were observed for magnetic samples based on HDTMA clays, indicating that Fe oxide synthesis does not significantly modify the size of the interlayer space of the organoclays. The determined d001 values for B50Mt, B100Mt, and B150Mt were 1.6 nm, 1.8 nm, and 2.0 nm, respectively, which indicates surfactant arrangements corresponding with monolayer for B50Mt, bilayer for B100Mt, and pseudo trilayer for B150Mt [27,28]. Depending on the layer charge (=interlayer cation density = packing density of the alkylammonium ions) of the clay mineral and the chain length of the organic ion, different arrangements of organic molecules between the layers can be formed. The geometry of the surface and the degree of exchange can also influence. The organic ions may lie flat on the silicate surface as a monolayer or bilayer or, depending on the packing density and the chain length, an inclined pseudo trilayer structure can be formed, with the chains radiating away from the silicate surface.

For HDTMA-based clays, the magnetic composites attained for BAC presented similar *d001* values to those of the organoclays, revealing that more surfactant molecules remained in the interlayer space after Fe oxide synthesis.

The TGA for both surfactants allowed us to observe that the actual organic content in the samples was lower than the concentration in the suspension, indicating that not all available surfactants were incorporated into the Mt surfaces. The mass loss percentage was determined from TGA data analysis, while the actual surfactant loading for all exchanged samples was calculated considering the mass loss of the MtMag structural hydroxyl groups. The actual values of % CEC of the organomagnetic samples were lower than the theoretical ones, calculated from the initial amount of HDTMABr applied. This behavior has been mainly attributed to two factors: incomplete exchange of HDTMA+ as observed for the actual CEC obtained for organic Mt, and increased release of surfactant during the synthesis of magnetic material, as previously determined [12].

In addition, a higher amount of surfactant incorporated in the synthesis implies a higher surfactant

Table 2. Hyperfine parameters extracted from Mössbauer spectra fittings

Sample	Paramagnetic sites								
	Fe^{3+}(I)			Fe^{3+}(II)			RP		
	δ	Δ	RSA	δ	Δ	RSA	δ	Δ	RSA
B50MtMag	$0.33_{0.20}$	$0.65_{0.0}$	10 ± 2	$0.39_{0.2}$	$1.88_{0.15}$	1 ± 1	$0.45_{0.10}$	$0.05_{7.86}$	33 ± 5
B100MtMag	$0.30_{0.19}$	$0.65_{0.27}$	9 ± 1	$0.35_{0.10}$	$1.70_{0.15}$	<1	$0.35_{0.1}$	$2.90_{10.66}$	25 ± 4
B150MtMag	$0.35_{0.08}$	$0.50_{0.16}$	7 ± 1	$0.30_{0.20}$	$1.15_{0.20}$	3 ± 1	$0.41_{3.33}$	$0.0_{7.25}$	21 ± 4

| Sample	Magnetic sites									
	Fe_3O_4 (A site)			Fe_3O_4 (B site)			α-FeOOH			
	δ	H	RSA	δ	H	RSA	δ	ε	H	RSA
B50MtMag	$0.36_{0.24}$	$47.5_{1.0}$	19 ± 3	$0.44_{0.25}$	$43.3_{2.2}$	30 ± 4	$0.43_{0.15}$	$-0.14_{0.1}$	$35.5_{2.0}$	7 ± 1
B100MtMag	$0.31_{0.17}$	$48.21_{0.8}$	31 ± 4	$0.55_{0.18}$	$44.9_{2.3}$	31 ± 4	$0.32_{0.00}$	$-0.14_{0.1}$	$36.6_{0.9}$	4 ± 1
B150MtMag	$0.30_{0.18}$	$48.1_{0.31}$	25 ± 4	$0.55_{0.28}$	$44.5_{2.1}$	40 ± 3	$0.43_{0.10}$	$-0.14_{0.1}$	$35.6_{2.0}$	4 ± 2

Symbols: δ, Δ, and ε represent the isomer shift, the quadrupole splitting, and the quadrupole shift, respectively, in mm/s, while H denotes the hyperfine magnetic field (*T*) and RSA the relative spectral area for each proposed Fe site.

content on the clay surface, but the contents calculated by TGA indicate that there is no saturation of the clay CEC with the amount of amine incorporated. For example, for the H50Mt sample, approximately 43% of amine was incorporated.

Considering the data of the actual load for organoclays and their magnetic counterparts, it can be noted that during Fe oxide synthesis, a minor part of the surfactant is lost, that is, more surfactant remains in the composites. The actual organic load obtained for both surfactants at equal concentrations seems to be similar for the two lower concentrations; however, in the case of 150% CEC, B150Mt presented a lower organic incorporation than H150Mt. This can be related to the structural characteristics of the BAC molecule, which presents a structure with two phenyl rings, while HDTMA presents a head-tail structure, with BAC higher than HDTMA. The small size of HDTMA makes its incorporation easier at relatively higher concentrations of Mt in BAC molecules. This hypothesis is also supported by evidence that the surfactant percentage on the interlayer was higher for HDTMA than for BAC. These differences in the Mt loading and their distribution could cause differences in the Fe content and magnetite formation in the composites, as revealed previously for HDTMA [12]. To analyze this issue, magnetic and hyperfine characterization of BAC samples was performed, as discussed below.

Figure 2 shows the Mössbauer spectra and the proposed fit for the magnetic organoclay obtained using BAC. The spectra for samples containing HDTMA have already been reported [11]. Six Fe environments were proposed (Table 2): two paramagnetic Fe^{3+} (called Fe^{3+}(I) and Fe^{3+}(II)), one associated with Fe in paramagnetic relaxation (PR), the two expected sites for magnetite (Fe_3O_4 A and B), and another corresponding to goethite (α-FeOOH).

Paramagnetic Fe^{3+} environments and paramagnetic relaxation can be associated with the presence of Mt [12], while magnetite and goethite are the Fe oxides synthesized during alkaline oxidation in the presence of nitrate. The relative spectral area (RSA) for magnetite was $49 \pm 5\%$ for B50MtMag, $62 \pm 6\%$ for B100MtMag, and $65 \pm 6\%$ for B150MtMag, while goethite presented values around 5% for all the samples. The ideal magnetite reveals a ratio between the RSA of the B and A sites of 1.8 [29], allowing us to conclude that the synthesized magnetite on the organoclays presented different grades of oxidation, owing to the obtained ratios for B50MtMag, B100MtMag, and B150MtMag, which were 1.58, 1.00, and 1.60, respectively. Based on these results and a previous report [29], the attained magnetite oxides on BAC samples present structural formulas of $Fe_{2.99}O_4$, $Fe_{2.92}O_4$, and $Fe_{2.96}O_4$ for B50MtMag, B100MtMag, and B150MtMag, respectively, and the oxidized form seems to be maghemite, with hyperfine parameters
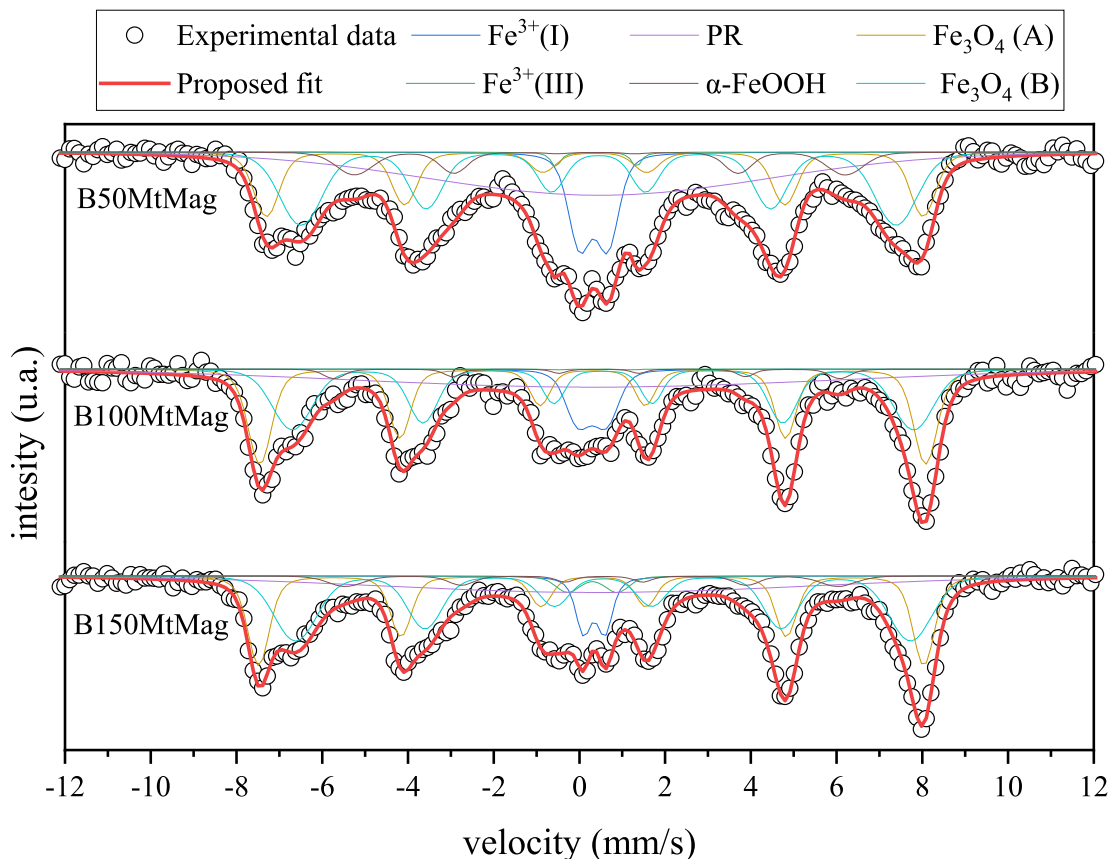
Figure 2. Mössbauer spectra of magnetic organoclays synthesized using BAC. Dots represent experimental data, and the red line is the resultant fit.

similar to magnetite and identical diffraction patterns.

The actual magnetite content was related to the magnetic response and was estimated by considering the total Fe concentration of each sample (Table 3). The total Fe concentration was determined from the Mössbauer spectra using the approximate method described previously [25]. The Fe concentrations associated with magnetite (Table 3) were similar for the three magnetic composites developed using BAC, whereas the values were lower than those reported for H50MtMag, H100MtMag, and H150MtMag of 134, 152, and 131 g/kg, respectively [11]. In the same work, it was concluded that the HDTMA molecules located on the internal surface of Mt would decrease the incorporation of Fe at that site, leaving more Fe atoms free for magnetite formation on the external surface of the clay. The Fe atoms on the inner surface of the clay do not favor magnetite formation. According to TGA analysis, the surfactant loading in the interlayer space is higher with HDTMA than with BAC for the same initial surfactant concentration. This result may be associated with the larger volume of BAC molecules than that of HDTMA. Similar interlayer Fe concentrations were determined for magnetic organoclays prepared from organoclays with the same initial surfactant concentration. Larger surfactant molecules could hinder Fe incorporation into the interlayer space. Thus, despite the lower BAC concentration in the interlayer space compared with HDTMA, the incorporation of Fe ions into the Mt interlayer space could be just as difficult, leaving Fe ions available for oxide formation. For the BAC-based magnetic compounds, the magnetite content (Table 3) was similar for all compounds, despite differences in Fe concentration.
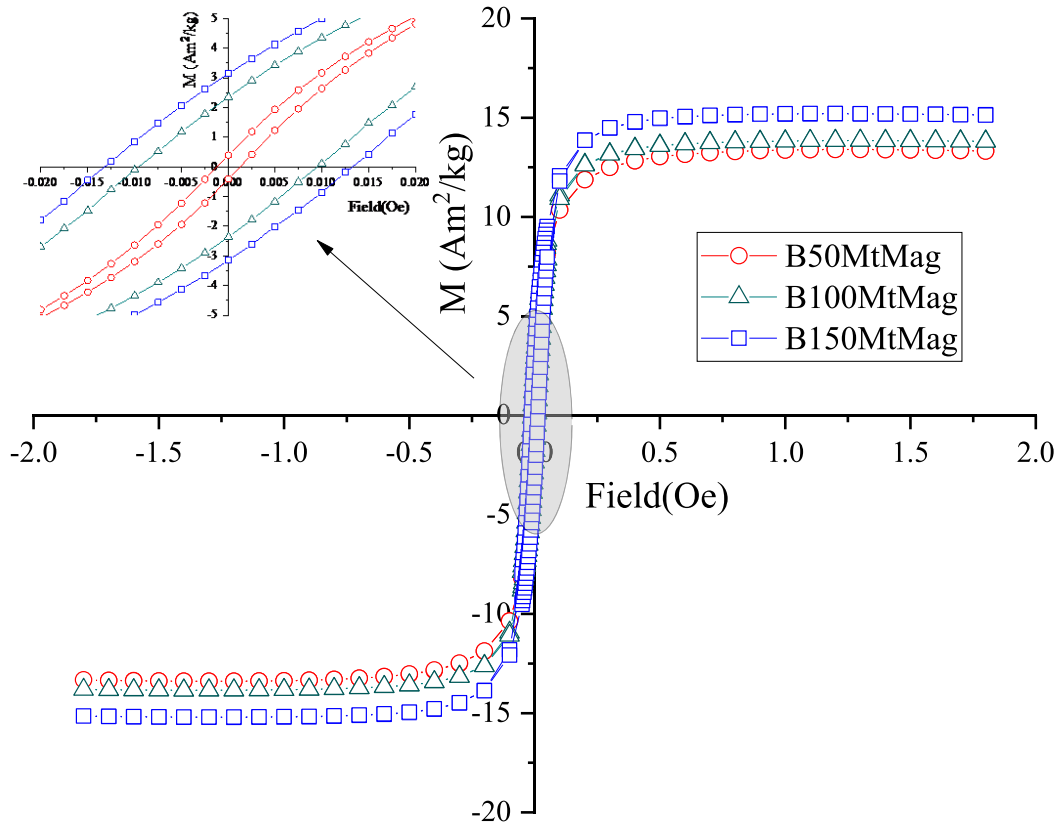
Figure 3. Hysteresis loops of magnetic organoclays obtained using BAC surfactant.

Table 3. Total Fe concentration, Fe in magnetite (Fe_3O_4), and magnetic parameters extracted from hysteresis loops: high field susceptibility, coercive field Hc, remanent magnetization Mr, and saturation magnetization Ms

Sample	Total Fe (g/kg)	Fe_3O_4 (%)	Fe in Fe_3O_4 (g/kg)	χ_{hifi} (10^{-7} m^3/kg)	Hc (mT)	Mr (A·m^2/kg)	Ms (A·m^2/kg)
BMt50Mag	206 ± 14	49 ± 5	100 ± 10	7.8 ± 0.5	2 ± 2	0.40 ± 0.10	13.5 ± 0.2
BMt100Mag	172 ± 20	62 ± 6	107 ± 13	4.5 ± 0.3	9 ± 2	2.36 ± 0.05	13.9 ± 0.2
BMt150Mag	166 ± 16	65 ± 5	108 ± 11	5.0 ± 0.3	14 ± 2	3.14 ± 0.02	15.3 ± 0.2

Note: Results for samples based on HDTMA were previously reported [11].

Going deeper into the magnetic characterization, Table 3 also presents the magnetic parameters extracted from hysteresis loops. The remnant magnetization and coercive field were determined for all samples, indicating hysteresis behavior and magnetite particles with sizes greater than 36 nm. In addition, the high field susceptibility, also observed for all samples, indicated the presence of particles with superparamagnetic behavior, that is, particles with sizes lower than 36 nm [30]. This result was observed in Figure 3. These observations have been previously reported for H50MtMag, H100MtMag, and H150MtMag samples, as well as for magnetite particles formed on beidellite clays [17] and a material composed of MtMag-hydrothermal carbon [11,19]. Saturation

magnetization determined for BAC samples resulted in 13.5 A·m^2/kg (BMt50Mag), 13.9 A·m^2/kg (BMt100Mag), and 15.3 A·m^2/kg (BMt150Mag). The higher value determined for BMt150Mag could be attributed to the fact that the magnetite formed on B150MtMag was less oxidized than that formed on B100MtMag. The saturation magnetization values obtained for all BAC-based organoclays suggest that they can be manipulated by an external magnetic field.

3.2. *Microdilution method and minimum inhibitory concentration (MIC)*

The results of the antimicrobial activity of organoclay against *E. faecium*, *E. coli*, and *S. typhimurium* using the microdilution method revealed with resazurin were used to determine the MIC (Table 4). Mt and MtMag did not present bactericidal activity as well as H50Mt, H50MtMag, B50Mt, and B50MtMag samples, probably because surfactant concentration was lower than the minimum necessary to have antibacterial activity in these cases. The aforementioned samples presented relatively low surfactant concentrations at the external surface (Table 1), which is the main factor responsible for the biocide characteristics of the clay [6]. The samples synthesized using surfactant concentrations equivalent to 100% CEC revealed variable behavior, whereas samples obtained at 150% CEC presented the highest bactericidal activity, in agreement with the higher concentration of surfactant at the external surface of the composites. Specifically, viable cells could not be detected with the H150Mt and H150MtMag sorbents at the concentrations assayed for all strains. In addition, it is important to highlight that H100MtMag, B100MtMag, H150MtMag, and B150MtMag presented biocide activity similar to that of non-magnetic variants, which allows the inclusion of iron oxides for manipulation with sorbent purposes without modifying the bactericidal activity. Among the microorganisms assayed, *E. coli* seemed to be the most susceptible to the biocide action of organoclays in all cases.

In conclusion, non-viable bacteria were detected in H150Mt and H150MtMag samples at all the concentrations tested. They became the most efficient system and were selected as the samples for assays in Erlenmeyer flasks.

Table 4. Minimum inhibitory concentration (MIC) for different samples in *E. coli, S. typhimurium*, and *E. faecium*

Sample	*E. coli* MIC (g/L)	*S. typhimurium* MIC (g/L)	*E. faecium* MIC (g/L)
Mt	ND*	ND*	ND*
MtMag	ND*	ND*	ND*
H50Mt	ND*	ND*	ND*
H50MtMag	ND*	ND*	ND*
H100Mt	1.25	10.0	10.0
H100MtMag	1.25	10.0	5.0
H150Mt	<0.625**	<0.625**	<0.625**
H150MtMag	<0.625**	<0.625**	<0.625**
B50Mt	ND*	ND*	ND*
B50MtMag	ND*	ND*	ND*
B100Mt	<0.625**	ND*	1.25
B100MtMag	<0.625**	ND*	ND*
B150Mt	<0.625**	1.25	<0.625**
B150MtMag	<0.625**	1.25	1.25

Notes: *ND means non-determinate cause in the experiment the highest clay concentration (10.0 g/L) could not inhibit bacterial growth. **<0.625 g/L means that bacterial growth could not be detected for the lowest concentration assayed in the experiment (0.625 g/L).

3.3. *Agar disk diffusion method*

This method is usually employed to determine the susceptibility of a bacterial strain to antimicrobial compounds. A clear zone, ring, or halo without bacterial development represents growth inhibition, which depends on the antimicrobial effectiveness of the compound, its concentration, and its ability to diffuse through the agar. Figure 4 shows bacterial lawns after incubation. It is possible to appreciate the absence of an inhibition halo in all cases. According to the microdilution method, the concentrations assayed (10 mg/mL) of H150Mt, H150MtMag, B150Mt, and B150MtMag were over the minimum value necessary to inhibit bacterial growth in liquid media. Therefore, they must be suspended and kept under constant stirring during water treatment to ensure intimate contact between them and bacteria. The fact that surfactants are not released into the water is an advantage, as if they were, they could be remnant pollutants.
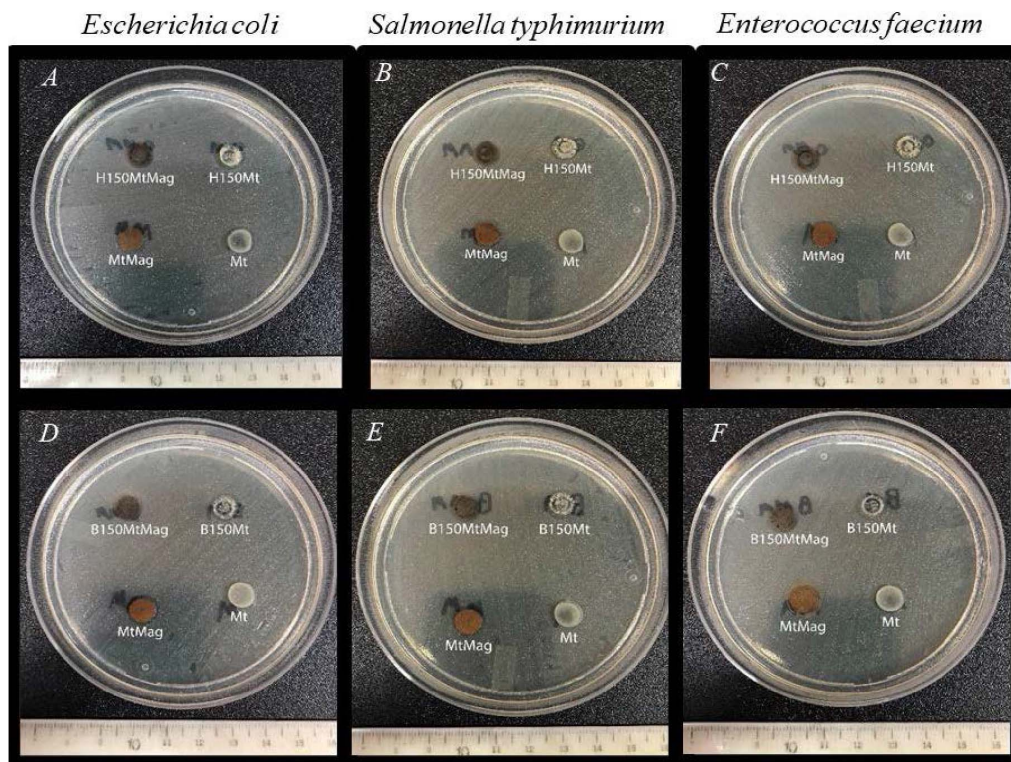
Figure 4. Plates employed in agar-disk diffusion method; samples assayed were (A–C) H150Mt, H150MtMag; (D–F) B150Mt, H150MtMag; controls assayed were (A–F) Mt, MtMag.

3.4. *Assays in Erlenmeyer flasks*

The present experiment was carried out with information provided by the microdilution method and MIC, which was used as a guide to determine which material concentration must be applied to ensure suitable growth inhibition. The results revealed that the most susceptible bacterium was *E. coli*; in agreement with the results of the microdilution method, a concentration of 0.25 mg/mL of material was required to cause bacterial inhibition in this case (Figure 5). The second one was *S. typhimurium* which required 0.50 mg/mL of material to be inhibited. The most resistant bacterial strain was *E. faecium* which required 0.80 mg/mL. Furthermore, there were no significant differences between H150Mt and H150MtMag; thus, the growth of Fe oxides did not affect the antibacterial activity of surfactant-loaded clays. This result indicates that this modification can be performed without damaging the biocidal properties of the compounds, with

the advantage of providing a magnetic response that can be used to remove the material relatively easily without direct contact after the remediation process.

4. Conclusions

Antimicrobial materials for water treatment were synthesized by modifying Argentine montmorillonite with hexadecyltrimethylammonium or benzalkonium chloride at different concentrations, with the posterior growth of Fe oxides. The chosen Fe oxide synthesis was adequate to impart a magnetic response to the biocide materials; only a small amount of surfactant was lost during the procedure, without significant antibacterial activity. The surfactant molecules were adsorbed on the external and internal surfaces of Mt. From an antimicrobial point of view, the surfactant located at the external surface is more relevant than that located at the internal surface; thus, the samples that showed higher surfactant presence on the external surface were those that were
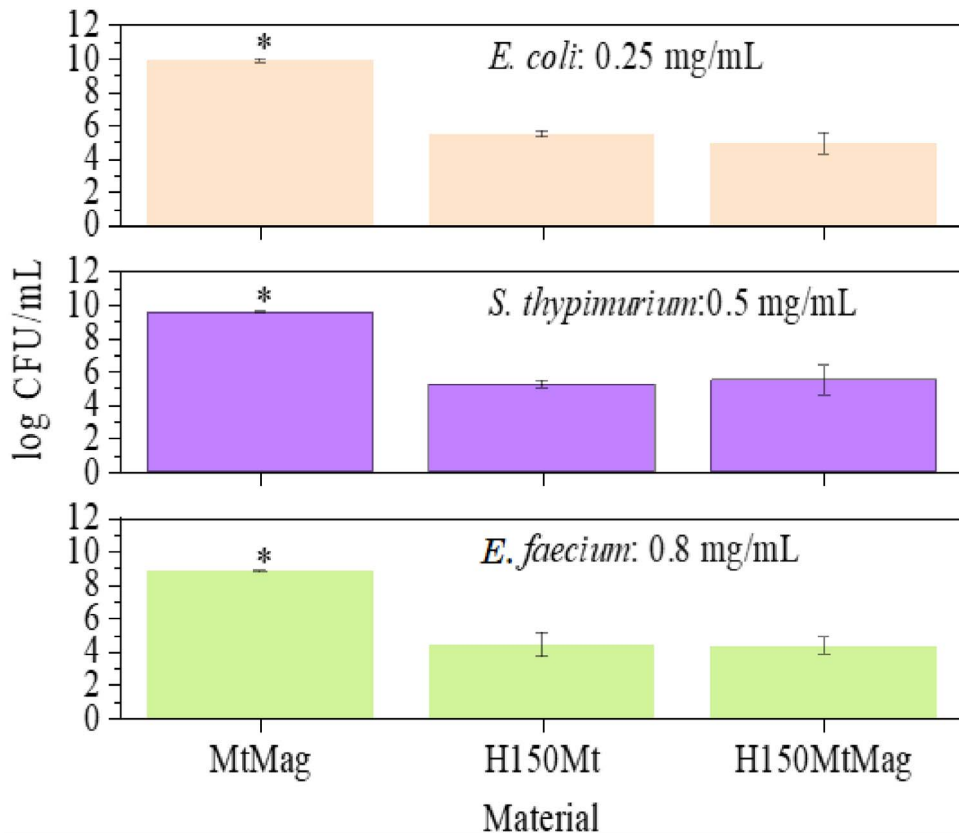
Figure 5. The number of viable bacteria for (A) assay against *E. coli* (material concentration 0.25 mg/mL, (B) assay against *S. typhimurium* (material concentration 0.50 mg/mL, and (C) assay against *E. faecium* (material concentration 0.80 mg/mL).

loaded with the highest surfactant concentrations. The material developed using the highest concentration of HDTMA had the highest surfactant load on the external surface, which is probably related to the smaller size of HDTMA compared to BAC. Magnetite was the main Fe oxide formed, and the saturation magnetization of all composites suggests adequate manipulation by an external magnetic field.

Although the Mt and MtMag samples did not show antimicrobial activity, the synthesized organoclays showed antimicrobial activity against bacteria. Among them, the sample with HDTMA as the organic source and a CEC load of 150 was the most efficient. The bacteria most susceptible to these materials were *E. coli*, *S. typhimurium*, and *E. faecium*, which were the most resistant. When the organoclays become magnetic, their antimicrobial activity remains, and the samples have an advantage: they can be recovered from the medium more easily than the non-magnetic ones, using an external magnetic field.

As a concluding remark, magnetic organoclays developed with a relatively high amount of HDTMA can be used as biocide materials for water treatment without releasing surfactants into the effluent. Therefore, it was possible to manipulate the mud derived from the treatment using an external magnetic field to separate the composites.

Declaration of interests

The authors do not work for, advise, own shares in, or receive funds from any organization that could benefit from this article, and have declared no affiliations other than their research organizations.

References

[1] M. Naseri, M. Maliha, M. Dehghani, G. P. Simon, W. Batchelor, *ACS Sens.*, 2022, **7**, 951-959.

[2] S. Buffet-Bataillon, P. Tattevin, M. Bonnaure-Mallet, A. Jolivet-Gougeon, *Int. J. Antimicrob. Agents*, 2012, **39**, 381-389.

[3] P. Herrera, R. C. Burghardt, T. D. Phillips, *Vet. Microbiol.*, 2000, **74**, 259-272.

[4] K. Malachová, P. Praus, Z. Pavlíčková, M. Turicová, *Appl. Clay Sci.*, 2009, **43**, 364-368.

[5] G. Özdemir, M. H. Limoncu, S. Yapar, *Appl. Clay Sci.*, 2010, **48**, 319-323.

[6] F. Yarza, C. F. Morantes, M. L. Montes, N. Bellotti, J. Salduondo, S. Yapar, F. Cravero, R. M. Torres Sánchez, *Mater. Chem. Phys.*, 2020, **253**, article no. 123390.

[7] J. Karasa, V. Nikolajeva, J. Kostjukovs, in *Presented at the 10th Baltic States Restorers' Triennial Meeting Seeking Balance: Preservation Use Conservation in Riga, Riga*, 2014.

[8] F. M. Flores, T. Undabeytia, M. Jaworski, E. Morillo, R. M. Torres Sánchez, *J. Environ. Chem. Eng.*, 2020, **8**, article no. 103806.

[9] M. Gamba, M. Olivelli, J. Lázaro-Martínez, G. Gaddi, G. Curutchet, R. Torres Sánchez, *Chem. Eng. J.*, 2017, **320**, 11-21.

[10] F. Barraqué, M. L. Montes, M. A. Fernández, R. Candal, R. M. Torres Sánchez, J. L. Marco-Brown, *Environ. Res.*, 2021, **192**, article no. 110247.

[11] F. Barraqué, M. L. Montes, M. A. Fernández, R. C. Mercader, R. Candal, R. M. Torre Sánchez, *Appl. Phys. A*, 2020, **126**, article no. 736.

[12] F. Barraqué, M. L. Montes, M. A. Fernández, R. C. Mercader, R. J. Candal, R. M. Torres Sánchez, *J. Magn. Magn. Mater.*, 2018, **466**, 376-384.

[13] T. Aydemir, S. Güler, *Artif. Cells Nanomed. Biotechnol.*, 2015, **43**, 425-432.

[14] G. Zhao, J. Wang, Y. Li, X. Chen, Y. Liu, *J. Phys. Chem. C*, 2011, **115**, 6350-6359.

[15] G. Fadillah, S. P. Yudha, S. Sagadevan, I. Fatimah, O. Muraza, *Open Chem.*, 2020, **18**, 1148-1166.

[16] X. Xu, W. Chen, S. Zong, X. Ren, D. Lui, *Chem. Eng. J.*, 2019, **373**, 140-149.

[17] M. L. Montes, F. Barraqué, A. L. Bursztyn Fuentes, M. A. Taylor, R. C. Mercader, J. Miehé-Brendlé, R. M. Torres Sánchez, *Mater. Chem. Phys.*, 2020, **245**, article no. 122760.

[18] J. Wang, Y. Chen, G. Liu, Y. Cao, *Compos. Part B Eng.*, 2017, **114**, 211-222.

[19] M. E. Z. Zelaya Soulé, F. Barraqué, C. F. Morantes, F. M. Flores, M. A. Fernández, R. M. T. Sánchez, M. L. Montes, *Materialia*, 2021, **15**, article no. 100973.

[20] X. Zhu, X. Fan, Y. Wang, Q. Zhai, M. Hu, S. Li, Y. Jiang, *Bioprocess Biosyst. Eng.*, 2021, **44**, 483-493.

[21] L. Chen, C. H. Zhou, S. Fiore, D. S. Tong, H. Zhang, C. S. Li, S. F. Ji, W. H. Yu, *Appl. Clay Sci.*, 2016, **127–128**, 143-163.

[22] M. Gamba, F. M. Flores, J. Madejová, R. M. Torres Sánchez, *Ind. Eng. Chem. Res.*, 2015, **54**, 1529-1538.

[23] H. Bartonkova, M. Mashlan, I. Medrik, D. Jancik, R. Zboril, *Chem. Pap.*, 2007, **61**, 413-416.

[24] K. Lagarec, D. Rancourt, *Recoil - Mössbauer Spectral Analysis Software for Windows*, University of Ottawa, Ottawa, 1998.

[25] M. L. Montes, P. C. Rivas, M. A. Taylor, R. C. Mercader, *J. Environ. Radioact.*, 2016, **162–163**, 113-117.

[26] M. Elshikh, S. Ahmed, S. Funston, P. Dunlop, M. McGaw, R. Marchant, I. M. Banat, *Biotechnol. Lett.*, 2016, **38**, 1015-1019.

[27] A. Meleshyn, C. Bunnenberg, *J. Phys. Chem. B*, 2006, **110**, 2271-2277.

[28] B. Schampera, D. Tunega, R. Šolc, S. K. Woche, R. Mikutta, R. Wirth, S. Dultz, G. Guggenberger, *J. Colloid Interface Sci.*, 2016, **478**, 188-200.

[29] R. E. Vandenberghe, E. De Grave, in *Mössbauer Spectroscopy: Tutorial Book* (Y. Yoshida, G. Langouche, eds.), Springer, Berlin, Heidelberg, 2013, 91-185.

[30] D. J. Dunlop, *J. Geophys. Res.*, 1973, **78**, 1780-1793.